

# Relationship between Ion Conductivity and Hierarchical Molecular Mobility of Oligocarbonate-based Electrolytes

Kojio, Ken

Institute for Materials Chemistry and Engineering, Kyushu University

Kaetsu, Katsuhiro

Graduate School of Engineering, Kyushu University

Hirai, Tomoyasu

Institute for Materials Chemistry and Engineering, Kyushu University

Takahara, Atsushi

K-NETs, Kyushu University

<https://hdl.handle.net/2324/7178800>

---

出版情報 : Chemistry Letters. 51 (4), pp.465-468, 2022-04-04. Oxford University Press (OUP)  
バージョン :  
権利関係 :



# Relationship between Ion Conductivity and Hierarchical Molecular Mobility of Oligocarbonate-based Electrolytes

Ken Kojio,<sup>\*1,2,3,4</sup> Katsuhiko Kaetsu<sup>2</sup>, Tomoyasu Hirai<sup>1</sup>, and Atsushi Takahara<sup>4</sup>

<sup>1</sup>Institute for Materials Chemistry and Engineering, <sup>2</sup>Graduate School of Engineering,

<sup>3</sup>WPI-FCNER, <sup>4</sup>K-NETs, Kyushu University.

744 Motooka, Nishi-ku, Fukuoka, 819-0395

E-mail: kojio@cstf.kyushu-u.ac.jp

To obtain a direction for an experimental design to clarify the ion conductivity mechanism, the effects of type of lithium salt, salt concentration, and number density of branching points on conductivity of aliphatic polycarbonate-based lithium-ion electrolytes were investigated using dielectric, conductive, and viscosity measurements. It was revealed that hierarchical molecular mobility including local, micro-, and macro-Brownian modes affect the conductivity of polymer electrolytes depending on the situation of electrolytes, such as salt concentration, type of salt, and molecular architecture.

**Keywords:** Ion conductivity | Molecular mobility | Oligocarbonate

Lithium-ion secondary batteries are attractive energy storage devices because of their largest energy density and voltage in the secondary battery family. However, organic electrolytes have a risk of leakage and explosion.<sup>1,2</sup> Polymer electrolytes have been considered as potential candidates to solve these issues because they exhibit stable and flexible properties. However, their conductivity is not sufficiently high.

Since the first report of poly(ethylene oxide) (PEO)-based electrolytes,<sup>3</sup> most attention of polymer-based electrolytes has been directed to polyethers.<sup>4-6</sup> The effects of chemical structure of polymers,<sup>7-9</sup> salt solubility,<sup>10</sup> inorganic fillers,<sup>11,12</sup> and organic-inorganic hybrids<sup>13-15</sup> on the conductivity of electrolytes have been examined, and conductivity at room temperature improved to the order of  $10^{-4}$  S cm<sup>-1</sup>. The polar ether oxygen induces dissociation of salt,<sup>4</sup> and the ionic motion in polyether-based electrolytes is cooperative with the molecular motion of polymer chains.<sup>4,16-25</sup> The ion conductivity can be increased with increasing salt concentration because of the increment of the number of carriers. However, after a certain salt concentration, the ion conductivity exhibits a reducing tendency because the mobility of polymer chains in the matrix is restricted by the strong interaction between lithium ions and ether oxygens. The lithium ions cross-link polyether chains by inter- and intra-chain binding through interaction of cationic charge and lone pairs in ether oxygen to restrict both global and local motions of the polymer chains. To improve the conductive property of the PEO-based electrolytes, some researches have been reported based on simulational and experimental methods.<sup>26-28</sup>

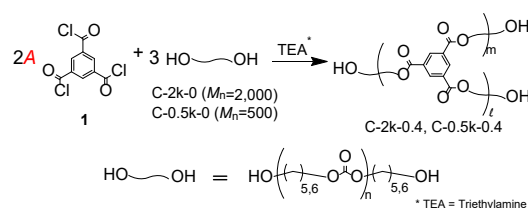
Aliphatic polycarbonate (PC)-based electrolyte is another possible polymer electrolyte for lithium ion batteries due to their high dipole moment and high solubility of lithium

salts.<sup>29-32</sup> Thus, PC-based electrolytes have potential to achieve further improvement of conductivity up to the practical level. Although linear aliphatic PC electrolytes have been investigated,<sup>29-36</sup> the mechanism of ion conductive behavior, including relationship between conductivity and chain architecture and molecular mobility of matrix polymers, the effect of the type of salt, and interaction between polymer chain and salts have not been clarified yet.<sup>35-37</sup> Polymer chain architectures affect both the local chain dynamics and viscosity and consequently, influence ion conductivity.

In this study, the effects of the type of lithium salt, salt concentration, and number density of branching points on conductivity of aliphatic oligocarbonate-based lithium-ion electrolytes were investigated based on molecular mobility analysis using dielectric, conductive, and viscosity measurements. Moreover, the relationship between hierarchical molecular mobility and conductivity was discussed based on these results.

Scheme 1 shows the synthetic procedure of the branched oligocarbonates. The A<sub>2</sub>B<sub>3</sub>-type hyper-branched oligocarbonates were prepared by the condensation reaction of trimesoyl chloride (**1**, Tokyo Chemical Industry Co., Ltd.) and aliphatic oligocarbonate glycols (Asahi-Kasei Chemicals Co.) with number average molecular weight ( $M_n$ ) of 2k or 0.5k. The last digit of the sample abbreviation is the ratio of [COCl] to [OH] in a feed mixture ( $A = [\text{COCl}]/[\text{OH}]$ ). The  $M_n$  and the number of terminal groups in a single branched oligocarbonate increase with an increase in  $A$ . To characterize the molecular structure of branched oligocarbonates, nuclear magnetic resonance (NMR) and size exclusion chromatography (SEC) were performed for purified samples.

Lithium perchlorate (LiClO<sub>4</sub>, Wako Pure Chemical Industries, Ltd.) or lithium bis(trifluoromethanesulfonyl)



**Scheme 1.** Synthesis of the branched oligocarbonate.  $A$  is the ratio of [COCl] to [OH] in a feed mixture ( $A = [\text{COCl}]/[\text{OH}]$ ). Abbreviation denotes molecular weight of oligocarbonate and  $A$ .

1 imide (LiTFSI, Tokyo Chemical Industry Co., Ltd.) were  
 2 used as a salt of the electrolytes. Lithium salt and linear  
 3 oligomers or newly synthesized branched oligomers were  
 4 dissolved in dimethyl carbonate, and the solution was dried  
 5 under vacuum at 333 K for 24 h to obtain electrolyte samples.  
 6 The abbreviation denotes the name of polymer, molecular  
 7 weight, molecular architecture (L: Linear, B, Branch),  
 8 concentration of salt [lithium salt] / [C=O], and type of Li-  
 9 salt (P: perchlorate, T: bis-(Trifluoromethane)  
 10 sulfonyl)imide).

11 To determine the glass transition temperature ( $T_g$ ) of  
 12 electrolytes, differential scanning calorimetry (DSC)  
 13 measurement was performed using a DSC 6220 (Seiko  
 14 Instruments Inc.) in the temperature range from 123 to 423 K  
 15 under dry  $N_2$  gas flow at a heating/cooling rate of 10 K  $min^{-1}$ .  
 16 The dynamic viscoelastic property of electrolytes was  
 17 measured by an oscillatory rheometer (Physica MCR 101,  
 18 Anton Paar GmbH) with strain amplitude range of 0.01-0.3%,  
 19 which was within the linear viscoelastic region during the  
 20 temperature range of 258 to 353 K. A cone plate (diameter  
 21 of 50 mm, cone angle of 1°, truncation spacing of 0.101 mm)  
 22 was used and the angular frequency was increased from 0.1  
 23 to 300  $rad\ s^{-1}$  in the temperature range from 258 to 353 K.  
 24 The zero-shear viscosity ( $\eta_0$ ) was determined by the  
 25 extrapolation of the plateau region in the frequency sweep  
 26 curve of real viscosity.

27 Measurements of conductivity and dielectric relaxation  
 28 of electrolytes were conducted using a Solartron 1260  
 29 impedance/gain-phase analyzer (Solartron Analytical)  
 30 equipped with a Solartron 1296 dielectric interface (Solartron  
 31 Analytical) under a He atmosphere, which is an inert gas with  
 32 high thermal conductivity. The sample was sandwiched  
 33 between a pair of 0.5  $cm^2$ -Au electrodes with a 50  $\mu m$ -  
 34 thickness spacer made of polyethylene terephthalate film, and  
 35 was placed in a LN-Z type cryostat (JECC TORISHA, Co.,  
 36 Ltd.) whose temperature was controlled within 93 to 353 K  
 37 using Lake Shore Model 311 temperature controller (Lake  
 38 Shore Cryotronics, Inc.). The measurement was conducted in  
 39 the frequency range of 0.01-10 MHz. The measurement  
 40 results were expressed in terms of either the complex  
 41 conductivity  $\sigma^* = \sigma' + i\sigma''$  or the complex permittivity  $\epsilon^* = \epsilon' + i\epsilon''$ .  
 42 The dc conductivity ( $\sigma$ ) and relaxation frequency  $f_k$   
 43 were determined by the extrapolation of the plateau region in  
 44 the frequency sweep curve of  $\sigma'$  and the Havriliak-Negami  
 45 equation fitting of the frequency sweep curve of  $\epsilon''$ .<sup>37</sup>

46 Figure 1 shows the salt concentration dependence of  $\eta_0$ ,  
 47  $T_g$ , and conductivity normalized with the salt molar  
 48 concentration ( $\sigma\sigma^{-1}$ ) of C-2k-L-based electrolytes with  
 49  $LiClO_4$  and LiTFSI.  $\eta_0$  and  $T_g$  of both electrolytes  
 50 monotonically increased with the increase in salt  
 51 concentration. This might be related to a decrease in the  
 52 degree of chain diffusion and segmental mobility of  
 53 oligocarbonates with an increase in salt concentration. These  
 54 will be discussed with the results of frequency and  
 55 temperature dependence of dielectric properties. On the  
 56 contrary,  $\sigma\sigma^{-1}$  increased and decreased at approximately  
 57 [lithium salt] / [C=O] = 0.14 with an increase in salt  
 58 concentration. Generally,  $\sigma$  is given by the following  
 59 equation,

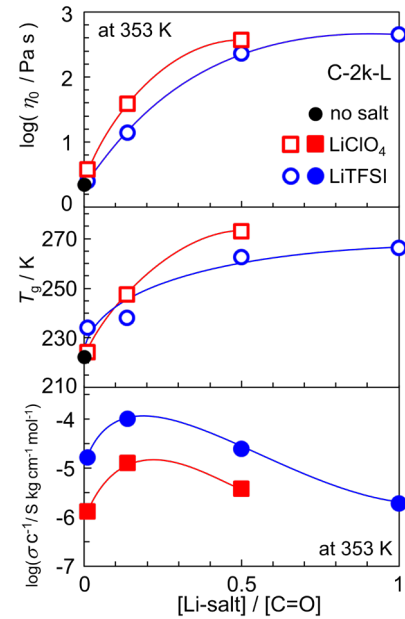


**Figure 1** Lithium salt concentration dependence of zero-shear viscosity  $\eta_0$  at 353 K, glass transition temperature  $T_g$ , and ion conductivity normalized with the salt molal concentration  $\sigma\sigma^{-1}$  at 353 K.

$$\sigma = N_{ion} e \mu_{ion}$$

60 where the  $N_{ion}$  is the number of ions per unit volume,  $e$  is the  
 61 charge of an electron, and  $\mu_{ion}$  is the mobility of ions. Hence,  
 62 it seems that effective  $N_{ion}$  increased monotonically at a low  
 63 salt concentration range ([lithium salt] / [C=O] < ca. 0.14) on  
 64 the assumption of complete dissociation of salt and in spite  
 65 of the restriction of mobility of matrix oligomer. Above a  
 66 certain concentration ([lithium salt] / [C=O] > ca. 0.14.), the  
 67 mobility reduced owing to a strong restriction of molecular  
 68 mobility.

69 Figure 2 shows angular frequency dependence of  
 70 permittivity of linear oligocarbonate (C-2k-L) and C-2k-L-  
 71 based electrolyte (C-2k-L-0.01-P, C-2k-L-0.14-P, C-2k-L-  
 72 0.5-P) with various salt concentrations of  $[LiClO_4]/[C=O]$   
 73 measured at 228 K. Two relaxations at 10 and 10<sup>5</sup> Hz for C-  
 74 2k-L were observed. These peaks can be assigned to segment  
 75 mode ( $\alpha$  mode) and local mode ( $\beta$  mode) of carbonate chains,  
 76 respectively. For electrolytes, the relaxation, which is slower  
 77 than that of the  $\alpha$  mode, was observed at a low frequency  
 78 region. This relaxation seems to be related to retarded  
 79 relaxation by interaction with  $LiClO_4$ , and is called  $\alpha_{slow}$ .  
 80 Furthermore, another slow relaxation peak was observed  
 81 between  $\alpha$  and  $\beta$  relaxations called  $\beta_{slow}$ .

82 Figure 3 shows the relaxation map for C-2k-L and C-  
 83 2k-L-based electrolytes with various  $LiClO_4$  concentrations.  
 84 C-2k-L shows two relaxations in the measured temperature  
 85 and frequency ranges. The relaxation observed at lower and  
 86 higher temperature regions exhibited Arrhenius-type and  
 87 Vogel-Fulcher-Tamman (VFT)-type temperature  
 88 dependences, respectively. Moreover, temperature range of  
 89 the relaxation at the higher temperature region was 218-243  
 90

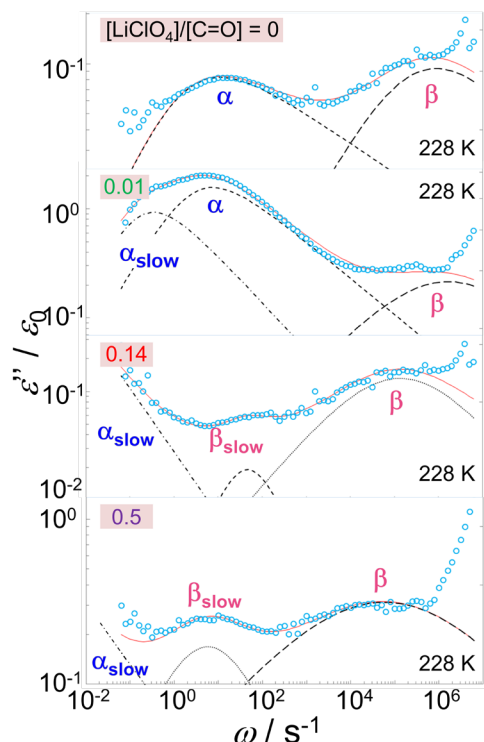


**Figure 2** Angular frequency dependence of permittivity of linear oligocarbonate (C-2k-L) and C-2k-L-based electrolyte (C-2k-L-0.01-P, C-2k-L-0.14-P, and C-2k-L-0.5-P) with various salt concentrations of  $[\text{LiClO}_4]/[\text{C}=\text{O}]$  measured at 228 K.

1 K, which is close to the  $T_g$  of C-2k-L. Therefore, these  
 2 relaxations were confirmed to be from local ( $\beta$ ) and  
 3 segmental motions ( $\alpha$ ), respectively. On the other hand, C-  
 4 2k-L-0.01-P, C-2k-L-0.14-P, C-2k-L-0.5-P showed three  
 5 relaxations, which had the lowest observation temperatures  
 6 in the measured range, slightly delayed with an increase in

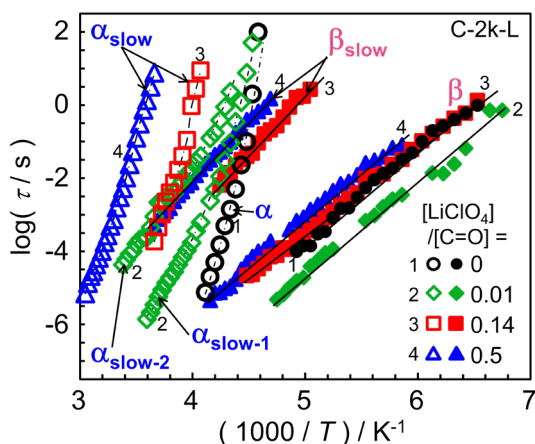


**Figure 3** Relaxation map of  $\alpha$  and  $\beta$  modes of C-2k-L, C-2k-L-0.01-P, C-2k-L-0.14-P, and C-2k-L-0.5-P obtained by dielectric measurement.

7 salt concentration, and resembled  $\beta$  relaxation of C-2k-L in  
 8 relaxation frequencies and temperature dependences.  
 9 Therefore, these relaxations were attributed to  $\beta$  relaxation.  
 10 The relaxations of C-2k-L-0.14-P, and C-2k-L-0.5-P, whose  
 11 observation temperatures were the second lowest in the  
 12 measured range, showed Arrhenius-type temperature  
 13 dependences. Thus, these relaxations were  $\beta$  relaxations  
 14 delayed by salt addition ( $\beta_{\text{slow}}$ ). The two relaxations of C-2k-  
 15 L-0.01-P were observed at temperature range of 223-273 K,  
 16 which is close to  $T_g$  of C-2k-L-0.01-P, and showed VFT-type  
 17 temperature dependence. Therefore, the lower temperature  
 18 relaxation was a slightly delayed  $\alpha$  relaxation ( $\alpha_{\text{slow-1}}$ ),  
 19 whereas the higher temperature relaxation was  $\alpha$  relaxation  
 20 highly delayed by salt addition ( $\alpha_{\text{slow-2}}$ ). The relaxations of C-  
 21 2k-L-0.14-P observed at the temperature range 245-273 K,  
 22 which is close to  $T_g$  of C-2k-L-0.14-P, showed VFT-type  
 23 temperature dependence. Therefore, these relaxations were  $\alpha$   
 24 relaxation delayed by salt addition ( $\alpha_{\text{slow}}$ ). Similarly, the  
 25 relaxation of C-2k-L-0.5-P observed at the temperature range  
 26 273-328 K, which is close to  $T_g$  of C-2k-L-0.5-P, would be  
 27  $\alpha_{\text{slow}}$  relaxation. The  $\alpha$  and  $\beta$  relaxations were delayed with  
 28 salt concentration leading to delayed relaxations ( $\alpha_{\text{slow-1}}$ ,  
 29  $\alpha_{\text{slow-2}}$ ,  $\alpha_{\text{slow}}$ ,  $\beta_{\text{slow}}$ ). The multi relaxation of electrolytes  
 30 indicates heterogeneous chain dynamics of the  
 31 oligocarbonate chains strongly coordinated and weakly  
 32 interacting with ions. Furthermore,  $\alpha_{\text{slow-1}}$  and  $\alpha_{\text{slow-2}}$  of C-2k-  
 33 L-0.01-P might be correlated with the  $\sigma c^{-1}$  increasing with  
 34 salt concentration in a low salt concentration range ( $[\text{LiClO}_4]$   
 35  $/ [\text{C}=\text{O}] < 0.14$ ).

36 The effect of the largest molecular mobility, macro-  
 37 Brownian motion, on the conductivity of oligocarbonate-  
 38 based electrolytes was also investigated. **Figures S1 and**  
 39 **S2** show NMR spectra and SEC curves of C-2k-L and C-0.5k-  
 40 B. These data provide information on the ratio of different  
 41 connecting states of end groups of C-2k-L and the size of the  
 42 isolated molecules in solvent, as presented in **Table S1**.  
 43 **Figure 4** summarizes the schematic representation of the  
 44 structure and size of C-2k-L and C-0.5k-B molecules. The  
 45 size of these two molecules were almost the same and the  
 46 chain density of C-0.5k-B was higher than that for C-2k-L.  
 47 Viscosity and conductivity measurements were performed  
 48 for polymer electrolytes of these two oligocarboxates with  
 49  $\text{LiClO}_4$ . **Figure S3** shows the temperature dependence of  
 50 ionic conductivity ( $\sigma$ ) and zero shear viscosity ( $\eta_0$ ) for C-2k-  
 51 L-0.14-P and C-0.5k-B-0.14-P. C-0.5k-B-0.14-P exhibited  
 52 higher conductivity and lower viscosity than C-2k-L-0.14-P.

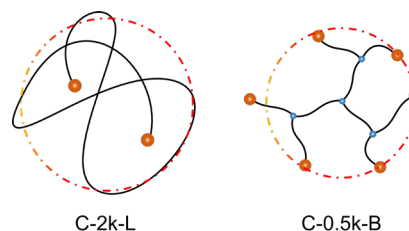


**Figure 4** Schematic illustration for random coil description of single molecular chain of C-2k-L and C-0.5k-B.



To investigate the temperature dependence for smaller molecular mobilities, dielectric measurements were carried out. **Figure S4** shows the relaxation map of  $\alpha$  and  $\beta$  modes of C-2k-L, C-2k-L-0.14-P, and C-0.5k-B-0.14-P ( $[\text{LiClO}_4]/[\text{C}=\text{O}] = 0.14$ ). C-0.5k-B-0.14-P had three relaxations. These relaxation frequencies and temperature dependences are almost the same as those of C-2k-L-0.14-P. Therefore, the difference between C-2k-L-0.14-P and C-0.5k-B-0.14-P in the local and segmental molecular mobilities is not significant. However, as shown in Figure S3, the  $\sigma$  values of C-0.5k-B-0.14-P and C-2k-L-0.14-P were  $4 \times 10^{-5} \text{ S cm}^{-1}$  and  $1 \times 10^{-5} \text{ S cm}^{-1}$  at 353 K, respectively. Moreover, the  $\eta_0$  values of C-0.5k-B-0.14-P and C-2k-L-0.14-P were 16 Pa s and 39 Pa s at 353 K, respectively. Therefore, the branching structure enhanced the chain diffusion to improve the conductivity even though the segmental and local mobilities had the same extent.

Finally, the effect of the size of salt was examined using two different salts. **Figure 5** shows the relaxation map of  $\alpha$  and  $\beta$  modes of C-2k-L-based electrolytes without and with  $\text{LiClO}_4$  and LiTFSI of  $[\text{LiClO}_4]/[\text{C}=\text{O}] = 0.14$ . When LiTFSI was used as a salt, the activation of molecular mobility was observed for  $\beta$  mode. Furthermore, the retardation of  $\alpha$  mode decreased for LiTFSI. Thus, LiTFSI may work to increase the conductivity of polymer electrolytes. This might be related to the volume induced by large counter ions of LiTFSI. These phenomena obtained in this study might be related to the increase in conductivity with increase in salt concentration observed by Tominaga et al.<sup>27</sup>

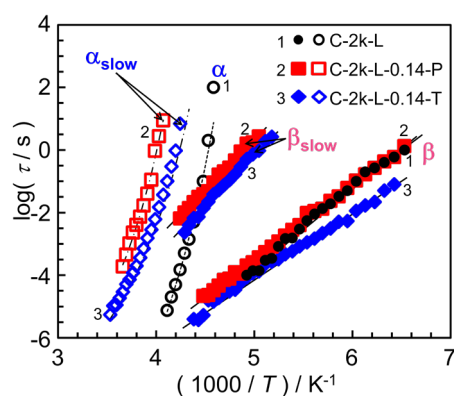


**Figure 5** Relaxation map of  $\alpha$  and  $\beta$  modes of linear oligocarbonate (C-2k-L)-based electrolytes without and with  $\text{LiClO}_4$  and LiTFSI of  $[\text{LiClO}_4]/[\text{C}=\text{O}] = 0.14$ .

In conclusion, hierarchical molecular mobility, local ( $\beta$  mode), micro- ( $\alpha$  mode), and macro-Brownian (viscosity) modes of carbonate chains affect the conductivity of polyelectrolyte depending on the situation of electrolytes, such as salt concentration, type of salt, and molecular architecture. These trends obtained with oligocarbonate-based electrolytes may lead to a significant increase in conductivity in comparison with polyether-based ones. To clarify the mechanism of ion conductivity of oligocarbonate electrolytes, further

investigation based on the results obtained in this study and measurement of the transference number are needed. Supporting Information is available on <http://dx.doi.org/10.1246/cl.220018>.

## References and Notes

- J.-M. Tarascon, M. Armand, *Nature* **2011**, 171-179.
- K. Xu, *Chem. Rev.* **2014**, *114*, 11503.
- D. E. Fenton, J. M. Parker, P. V. Wright, *Polymer* **1973**, *14*, 589.
- M. A. Ratner, D. F. Shriver, *Chem. Rev.* **1988**, *88*, 109.
- W. H. Meyer, *Adv. Mater.* **1998**, *10*, 439.
- J. Muldoon, C. B. Bucur, N. Boaretto, T. Gregory, V. Di Noto, *Polym. Rev.* **2015**, *55*, 208.
- S. Takeoka, H. Ohno, E. Tsuchida, *Polym. Adv. Technol.* **1993**, *4*, 53.
- M. Marcinek, J. Syzdek, M. Marczewski, M. Piszcz, L. Niedzicki, M. Kalita, A. Plewa-Marczewska, A. Bitner, P. Wiczorek, T. Trzeciak, *Solid State Ionics* **2015**, 276, 107.
- T. Itoh, N. Hirata, Z. Wen, M. Kubo, O. Yamamoto, *J. Power Sources* **2001**, *97*, 637.
- S. Sylla, J.-Y. Sanchez, M. Armand, *Electrochim. Acta* **1992**, *37*, 1699.
- F. Croce, G. Appetecchi, L. Persi, B. Scrosati, *Nature* **1998**, *394*, 456.
- F. Croce, L. Persi, B. Scrosati, F. Serraino-Fiory, E. Plichta, M. Hendrickson, *Electrochim. Acta* **2001**, *46*, 2457.
- T. Fujinami, A. Tokimune, M. A. Mehta, D. Shriver, G. C. Rawsky, *Chem. Mater.* **1997**, *9*, 2236.
- V. Münchow, V. Di Noto, E. Tondello, *Electrochim. Acta* **2000**, *45*, 1211.
- K. Shikina, H. Koike, Y. Tominaga, *Chem. Lett.* **2021**, *50*, 217.
- C. A. Angell, C. Liu, E. Sanchez, *Nature* **1993**, *362*, 137.
- A. Noda, M. Watanabe, *Electrochim. Acta* **2000**, *45*, 1265-.
- M. Watanabe, N. Ogata, *British Polym. J.* **1988**, *20*, 181.
- M. Watanabe, S. Aoki, K. Sanui, N. Ogata, *Polym. Adv. Technol.* **1993**, *4*, 179.
- A. Nishimoto, M. Watanabe, Y. Ikeda, S. Kohjiya, *Electrochim. Acta* **1998**, *43*, 1177.
- T. Furukawa, M. Imura, H. Yuruzume, *Jpn. J. Appl. Phys.* **1997**, *36*, 1119.
- K. Yoshida, H. Manabe, Y. Takahashi, T. Furukawa, *Electrochim. Acta* **2011**, *57*, 139.
- K. Timachova, H. Watanabe, N. P. Balsara, *Macromolecules* **2015**, *48*, 7882.
- K. Kojio, S. Jeon, S. Granick, *Euro. Phys. J. E*, **2002**, *8*, 167.
- J. Han, S. Takano, K. Fujii, *Chem. Lett.* **2021**, 50.
- K. Timachova, H. Watanabe, N. P. Balsara, *Macromolecules* **2015**, *48*, 7882.
- M. P. Rosenwinkel, M. Schonhoff, *J. Electrochem. Soc.* **2019**, *166*, A1977.
- N. Molinari, J. P. Mailoa, B. Kozinsky, *Chem. Mater.* **2018**, *30*, 6298.
- Y. Tominaga, K. Yamazaki, V. Nanthana, *ECS Transactions* **2014**, *62*, 151.
- Y. Tominaga, T. Shimomura, M. Nakamura, *Polymer* **2010**, *51*, 4295.
- Y. Tominaga, V. Nanthana, D. Tohyama, *Polym. J.* **2012**, *44*, 1155.
- J. Motomatsu, H. Kodama, T. Furukawa, Y. Tominaga, *Macromol. Chem. Phys.* **2015**, *216*, 1660.
- J. Mindemark, B. Sun, E. Törmä, D. Brandell, *J. Power Sources* **2015**, *298*, 166.
- S. D. Tillmann, P. Isken, A. Lex-Balducci, *J. Phys. Chem. C* **2015**, *119*, 14873.
- Y. Tominaga, *Polymer J.* **2017**, *49*, 291.
- K. Kojio, K. Kaetsu, T. Ohishi, T. Hirai, Y. Higaki, A. Takahara, The proceeding of International Congress on Rheology **2016**.
- S. Havriliak, S. Negami, *J. Polym. Sci. C* **1966**, *14*, 99.